Published by SET Publisher

Journal of Basic & Applied Sciences

ISSN (online): 1927-5129

Influence of Microstructure on the Dynamic Behaviour of Polyurethane Foam with Various Densities

Noureddine Boumdouha[1,2,*] and Mohamed Abderaouf Louar[2]

[1]*UMR CNRS 5223 Ingénierie des Matériaux Polymères, Université de Lyon, INSA Lyon, 20, Avenue Albert Einstein, 69621 Villeurbanne, France*

[2]*Laboratoire Dynamique des Systèmes Mécaniques, École Militaire Polytechnique, BP17 Bordj El-Bahri, 16046 Algiers, Algeria*

Article Info:

Keywords:
Polyurethane foam,
shock absorption,
optimum formulations,
static compression,
drop weight,
scanning electron microscopy.

Timeline:
Received: June 20, 2023
Accepted: July 21, 2023
Published: August 18, 2023

Citation: Boumdouha N, Louar MA. Influence of microstructure on the dynamic behaviour of polyurethane foam with various densities. J Basic Appl Sci 2023; 19: 131-150.

DOI: https://doi.org/10.29169/1927-5129.2023.19.12

*Corresponding Author
Tel: +213-697-005-578
E-mail: boumdouhanoureddine@gmail.com

Abstract:

Polyurethane foam is reinforced with varying proportions of metal loads and other components to increase shock absorption and mechanical impact. The main objective is to develop high-performance polymeric materials based on polyurethane foam developed with different compositions and specific densities. We monitor the growth distances and temperatures of the polyurethane foam in time to reach the optimum formulations. We conduct static compression tests and investigate the effect of drop weight on the deformation of polyurethane foam structures by dropping a weight from a specified height. Dynamic collisions cause deformations of the polyurethane foam structure. After investigating the low weight, we found that polyurethane foams have a good absorption coefficient at certain frequencies. Dynamic stress-strain response curves are used to characterize different stress rates. High-stress levels and similar strains indicate a high resistance to shock. We follow the evolution of microstructure structures by scanning electron microscopy (SEM) to observe deformation and fracture behavior with reversibility and recovery.

1. INTRODUCTION

The robot is among the most revolutionary technological innovations of recent years. Technological developments have made robots quicker, more intelligent, and smarter. With the increasing number of cameras, actuators, sensors, etc., modern robotics can utilize them. A few of these mechanical devices are touchy to applied stress or acceleration. Electronic equipment is expected to increase but remain safe in extreme environments. Using various types of elastic materials, scientists can make a sensor with different functionality [1]. We're looking for the best analytical for analyzing propriety viscoelastic and comparing them to experimentally determined values. This efficiency improvement could be accomplished by inserting the electronic equipment into polyurethane foam, which is also used to reduce impact and vibration loads. Polyurethane foam offers several dynamic characteristics with different performance characteristics [2].

Studies of these polyurethane foams are necessary because they can help engineers predict impact forces and peak retardation [3]. It is hard to calculate the forces using stresses caused by elastic wave stress [4]. Song and Dan K [5] have also studied the impact dynamics phenomenon by developing an impact model and forecasting the impact force. The elastomeric touchpad has a factor of linearity and stiffness in the contact area. In another function [6], the application of the contact platform was designed by nonlinear or linear contact hardness, and the effect varied [7]. The models can be analyzed to provide only the load pressure for various heights. However, most studies have not used physical properties (such as test specimens, drop mass, temperature, density, etc.) [8]. J. Sherwood and al. [9] studied the toughest workout of polyurethane foam to compressive power, which factored in temperature and the influence of density, strain rate, and strain. Researchers utilized viscoelastic equipment to defend digital systems during impact [10].

Wurtz synthesized the first urethane in 1849 [11]. Otto Bayer subsequently synthesized PUR in 1937 from the response of polyester double to diisocyanate [12]. This was also a significant development because it consisted of a novel way of polymerizing reactions under phase polymerization [13]. However, this polymer was initially considered useless [14]. Polyurethane is a polymer created by the response of hydroxyl groups and polyol groups to the isocyanate NCO groups and the resulting name of the urethane association [13-16].

Materials, including plastic foams, are solid-phase and gas-phase materials [17]. Thermoplastic foams can be rugged, elastomeric, or flexible. They can also be manufactured from a diverse variety of polymers like polystyrene, polyurethane, nitrile rubber, polyisocyanurate, polypropylene, polyethylene, polyvinyl chloride, ethylene-vinyl acetate, or even other polyolefins, and the global foam industry was dominated by poly In 2015, the global polymer foam industry totaled over $100 billion, with the production of 22 million tons as well as a projected consumption of 25 million tons in 2019 [18]. Polymeric foams will be the first preference as lighter materials whose properties can easily be tailor-made for various applications, including automobiles, furniture, footwear, space, toys, food, or building materials [19]. Polyurethane foam (PUR) is typically used for comfort or shock-resistant applications [16]. Polystyrene foams [20] are widely used for foodstuffs, sound and thermal insulation materials, and vinyl chloride poly foams. [21] for transport and building.

Polyurethane foams are pioneers in the industry focused on their excellent mechanical characteristics [22]. These include high elongation capacity, large resistance in warlike environments, large energy absorption aptitude, thermal stability, versatility in one's products and applications, chemical resistance, profitability, and ability to contribute to the final product's effectiveness and longevity [23, 24]. The work in 1937 of Bayer Otto and colleagues on IG Farben in Germany is one of the more notable achievements in PUR [25, 26]. The studies produced further evidence of the elastic characteristics of PUR.

Because of their high impact resistance deformities, low wave impedance, high distress absorption, etc., foam polyurethane has become one of the most widely used technologies in dynamic circumstances [27, 28]. They will play a major role in lowering the weight of defensive structures, adding to their high distinct strength (strength-to-weight ratio) while not reducing their capacity to weather, impact weight, or explosion shock. That will increase machinery mobility and increase safety and protection.

The chemical structure, crystallinity level, and crosslinking contribute to the foam's properties, including hardness, durability, cushioning, and tensile strength [29]. Coupling with reinforcing materials may

enhance the mechanical characteristics of the foam. Various strategies have been utilized to improve the impact strength of foam, including laminating [30, 31], sewing [32], and inserting fillers [14]. And various methods [33, 34]. Flexible foams provide strong pressure, likely energy, efficiency, and absorption of effects. Still, flexible foams have inferior cut and puncture resistance, resulting in their inability to dissipate energy under localized processing. The influence of reinforcing foam in dynamic load responses is investigated in the current study. The experiment included the creation of different foaming formulations and measuring their results during dynamic loading conditions. We perform tests to measure their relation to mechanical properties.

The quasi-static monitoring cannot be exploited to quantitatively evaluate the force absorption properties of polyurethane foams during shock absorber [35] only under settings where strain values are greater than those obtained utilizing traditional mechanical test capacities. For service environments that require shock reduction, what is required is a higher rating system that can obtain the complex reaction of the foam below loading rates, which more closely correlates to impact situations. The approach selected for the current research includes the usage of the drop weight effect tester. Based on the specimen structure and test design, the apparatus may be used to mimic a wide variety of experimental requirements. For example, the fracture resilience of a substance can be examined by analyzing the reaction of a sample to a load impact. Conversely, the tolerance of a substance to penetration may be analyzed with the help of sample plaques by a sharp or moderate head effect, depending on the type of study.

Characterizing the strength and impact characteristics of the polyurethane foam was important for the foam used for the weapon system [36]. The research was to investigate these three main areas. The first step was to evaluate the mechanical characteristics of polyurethane foam [36, 37]. Our second aim was to relate the energy absorption obtained from such calculations to a system that could be more realistic in a service setting. Finally, according to reports, the dynamic assessments of elastic modulus and elastic failure stress are associated with cell deformation [38]. The findings from the studies in this paper would serve as a foundation for developing polyurethane foams' mechanical and physical characteristics regarding relationships with current forms [39].

2. EXPERIMENTAL METHOD

2.1. Materials and Methods

2.1.1. Elaboration of Polyurethane Foams (PUR)

In manufacturing polyurethane foam, we used PMDI isocyanates featuring NCO reactive alcohol. We used aliphatic polyols, which include hydroxyl groups. This exothermic response results in the development of urethane groups, as defined in Figure **1** [16].

After conducting many experiments to create an ideal foam with shock-resistant properties, we devised an optimal formula for six samples that we assume have good chains of polyurethane foam, as shown in Figure **S3**. We tried to prove the results by experimental scientific methods. Some additives are listed in polyurethane foam, as shown in Table **1**, a method summary in the workflow diagram in Figure **S1**.

The expansion distance and temperature were reported at the site by making various polyurethane sample formulas (see Figure **2a**). For Ep_01, Ep_06, which was free of both bentonite and alumina loads, and Ep_04, which contained a small percentage of bentonite, we noticed a continuation of the restraint time following the mixing of both constituents A and B (See Figure **S1**), about 172 seconds. After that period,

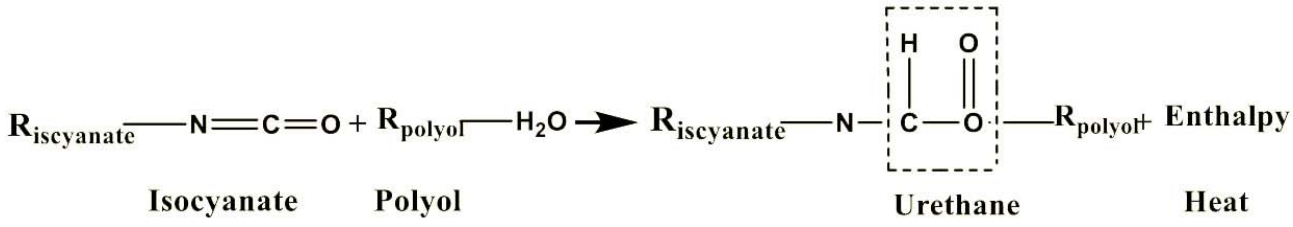

Figure 1: Urethane processing reaction scheme.

Were

$\mathbf{R_{isocyanate}}$ is produced from the monomer of isocyanate.

$\mathbf{R_{polyol}}$ is a polyol component derived from PU.

Table 1: Basic Compounds in the Preparation of Polyurethane Foams (in wt.%)

Samples	Ep_01	Ep_02	Ep_ 03	Ep_04	Ep_05	Ep_06
Polyol (POPE)	62.58	59.09	58.44	62.17	58.83	65.94
PMDI	32.29	24.87	26.26	29.49	24.09	26.61
Glycerin (GCO)	1.38	2.19	2.15	2.29	2.28	1.015
Dichloro-methane	0.74	0	0	0	1.24	0.82
Catalyst	0.93	1.25	1.251	0.97	1.89	1.74
Silicone (HS)	0.83	2.08	1.469	1.56	1.14	2.765
PEG	1.25	0	0	0	0	1.11
Bentonite BNT	0	10.52	10.43	3.52	0	0
Alumina Al_2O_3	0	0	0	0	10.53	0

a sharp rise in foaming was achieved, which lasted an average of a full minute and produced a final height of 19.1 cm. For me, Ep_02, Ep_03, and Ep_05, we noticed that it took time with significant loads. Over 10% had a more excellent restraint time of about 343 seconds, and the last height of 17.2 cm was measured after about 60 seconds.

In situ, temperature proportions are stated in Figure **2b**. About the situations of Ep_01, Ep_04, and Ep_06, perfectly of the restraint period before the onset of temperature rises right to polymerization, foaming occurred simultaneously with the foam expansion as anticipated. The main variance between the load-rich samples and those without the loads was related to the highest temperature achieved later in the reaction. For the samples Ep_02, Ep_03, Ep_05, the temperature was somewhat lower (3.6 °C +/-0.9 °C) than for the samples Ep_01, Ep_04, and Ep_06.

We can conclude that bentonite and alumina act as inhibiting. This has also been observed in some previous research [40], bentonite can stimulate relevant changes in the polyurethane microstructure, and these modifications can be inferred from measurements of in situ temperature. It is well-known that during the swelling of the foam, there is a match between the crystallization and blowing responses, which identifies the micro-structure of the polyurethane foam [41]. The alumina increased the damping time as it slightly reduced the heat expulsion of the reaction. Simply put, the loads acted as an animator, altering the fine structure of the polyurethane foam without significantly altering its chemical character.

The production of PUR in free expansion mode, that is to say, at atmospheric pressure, is carried out using a reactor with a volume of 300 ml and a mechanical stirrer with a speed of 2500 rpm. After thickening the PUR and cooling, it is extracted from the mold. The

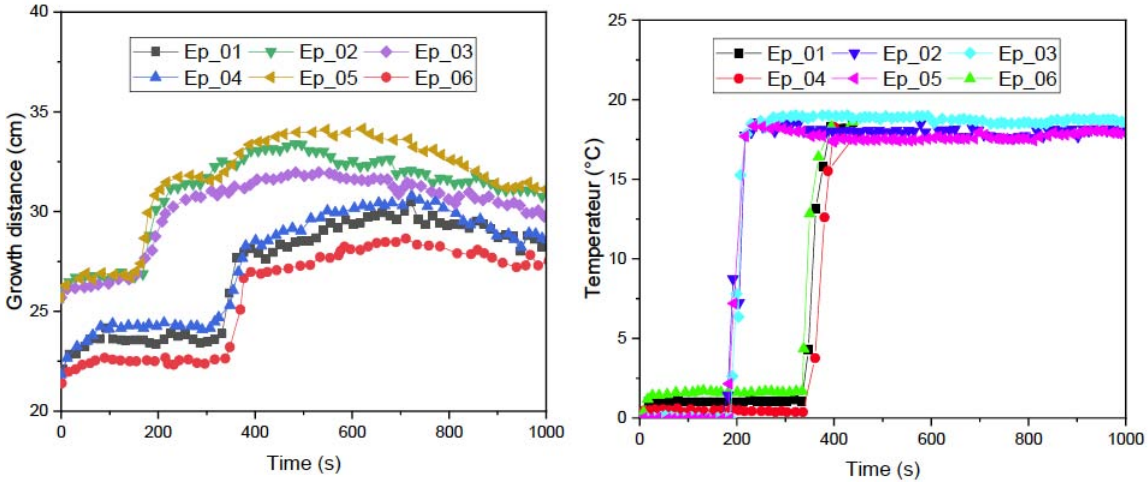

a b

Figure 2: Growth distances and temperatures for polyurethane foams as influenced by time.

a b c

Figure 3: The photo shows how homogeneous the polyurethane foam is after free expansion in free air.

effect is a foam that has, as seen in Figure **3a**, **b**, and **c**. Manual polishing method using the EcoMet ™ 30 polishing machine, as seen in Figure **S9**.

When preparing polyurethane foams, we strive to develop an optimal formula in which the final product has the necessary shock-absorbing properties [42]. Every time we fix the amount of polyols, isocyanates, and some additives, we gradually change the number of loads. We aim to determine the value of bentonite and alumina additives and loads for which the foam is more flexible and effective. Every time we ensure that the foam indicator is homogeneous, symmetrical, and consistent, we divide the foam into two parts with a sharp scalpel, check for the absence of defects, and note the distribution of loads inside the polyurethane foam core. Some samples of polyurethane foams of interesting formulas, as shown in Figure **S13**.

2.2. Dynamic Characterization

2.2.1. Drop Weight Tests

A test system given in Figure **4** was developed from [43] to carry out a dynamic compressive test. Effect checks were performed according to the recommendations of the NF EN ISO 6603-2 standard. For these dynamic tests, free drop weight is used without initial velocity on a specimen placed at its base. It is equipped with a steel impactor that has a square shape. The mass of the overall weight decline is 5 kg, and the maximum drop weight height is 1.20 meters. The latter is equipped with a sensor piezoelectric force type PCB 203B, with an acquisition card whose role is to bind the sensor with the digital oscilloscope with a bandwidth of 200MHZ, which is sufficient because of the test time, and a color screen and a USB input for data backup, to recover the forces exerted during the impact tests as a function of time. These measures are used to analyze the evolution of the strength and duration of the impact. The configuration of the test by impact tower is given in Figure **S10**.

The impact examination showed the polyurethane foam results for impact from the perpendicular position. Testing was performed by lowering the sample onto a flat surface to assess the effect yield as per ASTM D5628. The data was collected by exploiting Newton's laws (N) but was analyzed using DEWE Soft edition 6.5. The data was collected using a graphing technique with frequency in Hertz (Hz) and force in newtons (N). Piezoelectric sensors were used to measure the intensity of the impact directly after the impact. The system has intense sensitivity and is thus highly susceptible to interference patterns. To calculate the impact intensity, we calculated the maximum force peak.

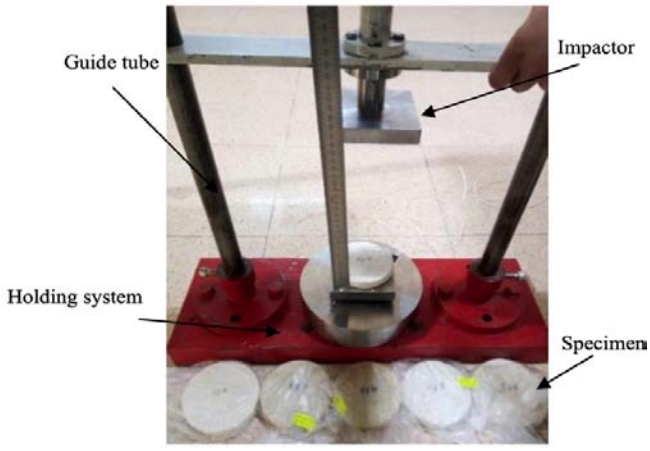

Figure 4: The image shows the drop weight exam and impact test specimen.

During the tests, we should assume temperature and humidity must be kept stable since they significantly influence the mechanical characteristics of polyurethane foam [43]. At least 10 minutes should lapse between repeats of impact tests as the viscoelastic repose of the polyurethane foam sample

Table 2: Characteristics of Drop Weight Tests

Samples	Length (cm)	Diameter (cm)	Density (g/cm^3)
Ep_1	1.09	10.09	0.43
Ep_2	1.02	10.05	0.15
Ep_3	1.05	10.09	0.27
Ep_4	1	10.07	0.30
Ep_5	1.08	10	0.22
Ep_6	1.06	10.06	0.38

can take as long. The recovery rate of the foam samples was measured after each test, where the recovery rate is defined as the ratio of the recovered height to the initial height of the foam sample.

The cylindrical specimen is about 1 cm long and 10 cm in diameter, prepared with different formulations using a special mold to prepare different sample dimensions for drop weight tests to maximize the free drop weight contact area. Fall weight test sample characteristics, as seen in Table **2**.

The effect experiments were performed on a drop weight tester attached to an automated data acquisition device. The testing frame may either be powered by gravity or mechanical control. In the case of the energy that could be transmitted to a research specimen greater than 300 J, energy could be transmitted to a velocity impact of around 840 J.

A faster data acquisition device that captures the performance of instruments has a high resolution of 1 Ps and can obtain a completed loading event in as little as approximately 4 ms. The program detects the difference in the crosshead rate among successive point data and analyzes the change. The energy absorbed by a specimen is then calculated from that instantaneous force and the measurement of the time derivative of the velocity since the crosshead is when the polyurethane foam sample is compressed.

The resilience measure is the resilience effect on the surface of the samples on which a hammer drops vertically. Though the entire structure of polyurethane foam is reinforced after applying reinforcing additives, the low-weight mallet has less impact load, which explains the effective difference between the two strengthening additives, alumina, and bentonite. The explanation is that the small effect thickness (approximately 10 cm) has fewer reinforcing additives and spray materials during manufacture. On the one hand, fewer sprayers produced smaller binding points throughout the reaction, but then again, a smaller percentage of reinforcing additives induced evenness of dispersion. The smaller polyurethane foam thickness was less rigid for these two factors than the broader thickness, and the impact resistance of the 10 mm thick PU foam with a lower solidity when exposed to the falling tower impact force.

After the preparation, we cut the samples into the milling machine by rotating the cutting tool (see Figure **S5**) on the one hand and the advance of the workpiece on the other hand, as given in Figure **S8**. The machine is equipped with numerical control to realize all complex forms, as shown in Figure **S5**. The specimens are loose during an impact according to Standard AITM 1-0010, as given in Figure **S6**.

The free drop weight test is used to study the bearing capacity of samples manufactured from polyurethane foam for the applied energy and their degree of absorption. To obtain some impact energy, E impact, the potential energy of the impactor is transformed into kinetic energy. The initial distance “H” between the upper roof of the specimen and the end of the impactor is calculated by:

$$H = 1.1\frac{E_{impactor}}{g * M_{impact}} \quad (1)$$

Where g is gravity = 9.81 m/s^2. The mass of the impactor “, M_{impact}.” is 5 kg, while factor 1.1 is used to compensate for the losses occurring during the test, such as the friction between the guide tube and the assembly of the drop weight.

For the acquisition of signals, a digital oscilloscope is used. For each input signal, a particular voltage range is set. The test is very fast and offers a wide group of frequencies. Thus, the frequency range of the acquisition system is set at its maximum of 200 kHz;

with each Δt = 0.005 ms, the values are recorded. This interval is very short (a few milliseconds), so a trigger associated with the signal of the force is used for signal recording. When a certain threshold is exceeded, the data backup is performed. The acquisition system can also save pre-trigger data, making all relevant data available. The test can be analyzed with the data collected during the impact. The first parameter to be determined is the impact force acting simultaneously on the impactor and the specimen. The force sensor delivers a voltage equal to the force in KN, 1V = 1KN.

2.3. Quasi-Static Characterization

2.3.1. Compression Tests

Six sets of samples were tested in compression quasi-static. Each series consists of four similarly shaped cylindrical specimens made from known formulations and compressed between the two compression plates of the apparatus until some deformation has been obtained. The stress difference for a sample strain is determined via a force transducer and reported during strain. Analysis of the data reveals the stress values versus demonstrating the stress-strain detour. The apparatus used for the compression tests is a 40 T dynamometer, which can be used in tension and compression. The mechanical compression tests were performed according to standard ASTM D3574 [44]. This test compresses the sample to 80% of its specific thickness at a 2 mm/min displacement. Compression should be maintained for 900 seconds. The stress curve and the final stress value are reported after 60 seconds, defined as compressive strength. The acquisition software calculates the value of Young's modulus according to Hooke's law, which measures stress and is then applied and recorded strain. This system is controlled by a computer that allows the start of the tests and acquisition of the data using the Merlin software, which makes it possible to program complex cycles and to follow the tests at different speeds or displacement control, according to Gibson and Ashby [45]. It is recommended to use engineering constants when analyzing the stress-strain response of foams, even up to enormous strains. To this end, we, therefore, measured the dimensions of each test piece just before and after the test.

2.4. Microstructural Characterization

2.4.1. Scanning Electron Microscope (SEM)

The microstructure and cell dimensions of foam polyurethanes are described by SEM (scanning electron microscope) type JEOL ALGS 840 with a 10 kV filament voltage. First, the specimens are broken down in nitrogen liquid. The breakage surfaces are gold-coated to conduct, and the collected micrograms are processed using the Scion Image software to calculate the space distribution in the foam polyurethane. Based upon the discretion of the radius dispensation of the disks measured in the images, the Saltikov technique [46] is used to determine the actual breadth of the space, assuming it's spherical.

3. RESULTS AND DISCUSSION

3.1. Dynamic Characterization

3.1.1. Drop Weight

The drop weight test is a dynamic validation for material behavior laws. The stress result curves were a feature of the crushing pace of the sample (obtained by processing the impactor displacement signal). For a better reading, the data is presented in absolute value. The piezoelectric sensor has a sensitivity of 56.2 mv per 1 KN, hence the need to process the results obtained from the oscilloscope by LabVIEW software being used to log details and true curves of the evolution of the power in terms of time. Figure **5** represents the behavior of the impact force, such as how it evolves with time for six impact energies obtained on six polyurethane foam samples. It can be seen that for impact energies lower than 15 J.

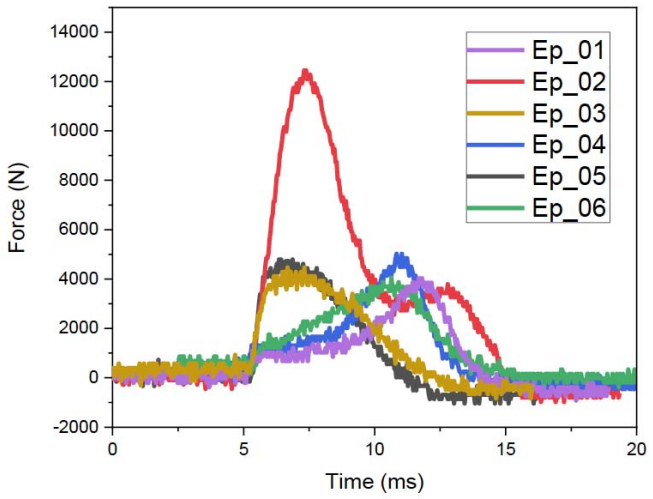

Figure 5: Characteristic force-time curve of polyurethane foams.

The development of the impact force is shown as a variable of the displacement. Until the displacement at the beginning of the application of the force on the sample, the force increases linearly with the

Table 3: Impact Forces and Corresponding Velocities for Specimens

Samples	V Impact velocity (ms^{-1})	V_{exp} (ms^{-1})	F_{max} (N)
Ep_1	3	3.1	5000
Ep_2	3.2	3.2	13000
Ep_3	3.4	3.5	5500
Ep_4	3.6	3.6	5000
Ep_5	3.8	3.9	5500
Ep_6	4	4.1	3800

displacement of the impactor, where there is high shock absorption resistance by polyurethane foam. The stiffness of the samples decreased while performing dynamic tests to assess the foaming behavior upon collision. As we recorded a maximum force resistance of about 1300 N/ms for sample Ep_2, we conclude that the greater the strength and pulse duration, the stronger the sample, as shown in Figure **5**.

By studying the temporal evolution of the energy transferred during the impact test of the cylindrical laminated polyurethane foam, we note that the energy of the foam increases to a maximum value equal to the kinetic energy. Based on the first results of the impact tests (force and time curves) associated with a visual inspection of the affected samples. The different energies and corresponding velocities are shown in Table **3**.

Table **3** shows that the test piece Ep_2 has better resistance to stronger influences than the rest of the samples, followed by Ep_3 and Ep_5, then Ep_1, Ep_4, and Ep_6. Using the values of the impact velocity measured by the sensor, and the experimentally computed velocity, it is possible to estimate the initial deformation velocities under the influence of the collider (here, we take into account the deformation rate of the initial contact point between the collider and the sample, and thus lies on the collider symmetry axis) are 170 s^{-1} for a drop height of 330 mm. It was found that the impact velocities had little influence on the obtained compression/crush curves, and the consistent result gave a range of redistributed contrast. However, the presented results should be taken with great care of the applied strength value and the sample dimensions, as a thickness greater than 10 mm corresponds to an increase of more than 33% of the compressive and crushing capacity. Indeed, due to the observed diversity in the results, the proposed curves appear significant in studying them.

We note that the results obtained match the formulas of the manufactured samples. The samples containing the loads have a great effect on shock absorption, as we find that the test samples have proven their worth in dynamic characterization, with the possibility of highlighting the fierce nature of the typical behavior of viscous elastic materials, due to their strong dependence on the rate of deformation coefficient (especially the increase in the value of Young and the response of the substance in terms of stress with an increase of $\dot{\varepsilon}_0$).

Table **4** shows the characteristics of the tests with the drop weight for the studied polyurethane foam samples. We note that the density of the samples is maintained before and after the test, as well as the velocity of deformation. Despite the collision, they

Table 4: Characteristics of Tests with Drop Weight for the Whole Sample

The samples	Length (mm)	Length after impact (mm)	Diameter (mm)	Diameter after impact (mm)	Density (g / cm^3)	Density after impact (g / cm^3)	Deformation speed, (s^{-1})
Ep_1_1	17.5	17.52	109.5	109.52	0.43	0.43	0.23
Ep_2_1	16.72	16.71	96.2	96.25	0.15	0.15	0.23
Ep_3_1	16.31	16.3	110.7	110.72	0.27	0.27	0.24
Ep_4_1	16.36	16.34	102.4	102.42	0.3	0.3	0.25
Ep_5_1	16.16	16.14	111.1	111.13	0.22	0.22	0.24
Ep_6_1	16.58	16.54	106.6	106.66	0.38	0.38	0.24

indicate that the samples remained preserved in their morphology. This will help us in non-lethal projectile applications [47]. In addition to the formation being simple, these foams are recoverable and reused.

The energy of the incident impact depends on the sample's location, the drop load's height, the force of gravity, and the recorded weight [48]. Although the impact energy and impact forces are not directly computed from the measured value, they can be determined by the applied forces. The weight of polyurethane foam is higher as the load fraction increases of both bentonite and alumina loads, indicating that the density of the polyurethane foam specimen is also relevant to the dimensions of the foam. The impact strength is expected to increase with the increase in the loading height.

3.2. Quasi-Static Characterization

3.2.1. Compression Tests

Static compression of the first Ep_01 foam collection is given in Figure **6** shows a sample placed between two plates on a test machine, showing how a static pressure test is performed by performing a forcible change of the polyurethane initial foam diameter of 35.5 mm. A small dispersion exists between the four test parts performed under the same processing and testing conditions. The force-displacement behavior of the first crystalline foam appears similar to that of the second, which consists of four samples. To ensure the uniformity of the structure of the various samples, we note that the curves are close and have the same behavior, which includes three phases, but with a difference in force as we apply a maximum force of 4000 newtons. We notice that the plateau starts at a great value of 500 Newtons and increases rapidly to 1500 Newtons. This behavior shows strength and endurance equivalent to that of heavy metals, which proves how hard the sample is. The most exciting thing is the return of the normal shape of the sample after a pressure process of more than 80 % of its original shape.

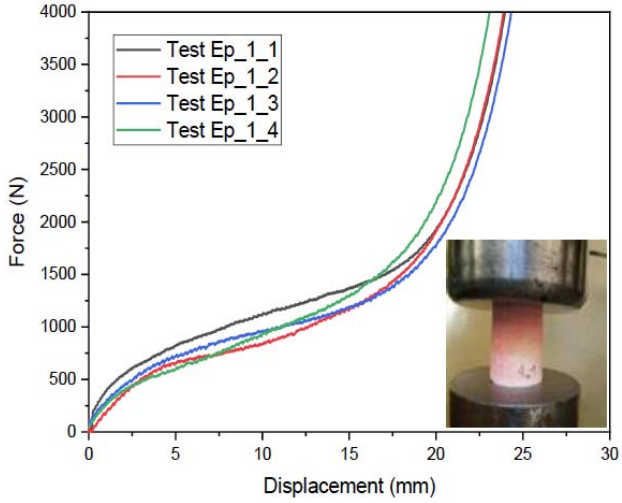

Figure 6: Force-displacement curve of polyurethane foams EP_01.

The axial pressure drains the second foam with a diameter of 34.72 mm. The Ep_02 force-displacement behavior shown in Figure **7** is three-phased, close to traditional framing, and allows for exponential behavior of the curves. Other authors [49-51] reported this behavior. The force-displacement curves overlay with an increase in the force being applied to the plane on the order of 200 N, although the force of 200 N is small for the plane relative to the first study. This shows its elasticity, and here we can infer that the force increases dramatically with the transformation compression rate.

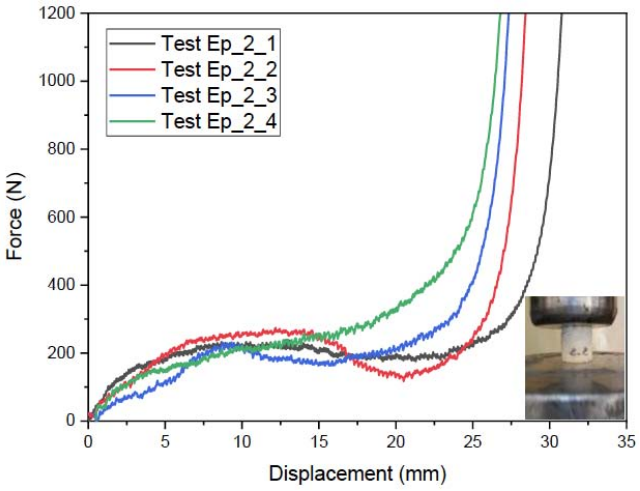

Figure 7: Force-displacement curve of polyurethane foams EP_02.

As for the curve of the third sample, measuring approximately 32,31 mm in diameter (Figure **8**), there is a scattering across the area where the force change ranges from 200 to 500 Newtons. This action illustrates how the pressure level is transformed. The force-displacement curve indicates an improvement of up to 4000 N as the maximum value compared to other types at a maximum force of 80 % load.

The fourth polyurethane open-cell foam, denser by 0,23 g/cm^3 than the second (EP_02), 0,08 g/cm^3, has the same three-phase compartment as the elastic and condensing plateau (Figure **9**). Due to the forced displacement behavior of this 32,4 mm foam, the

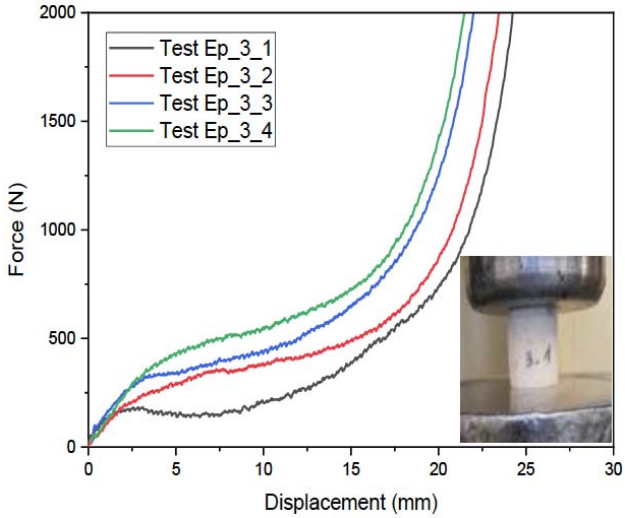

Figure 8: Force-displacement curve of polyurethane foams EP_03.

dispersion is much less than in the third foam (see Figure **8**), so the tests are relatively often. It also has a plateau force of about 500 Newtons, while the second foam is only 200 Newtons, and the maximum pressure of 80 % is 4000 N.

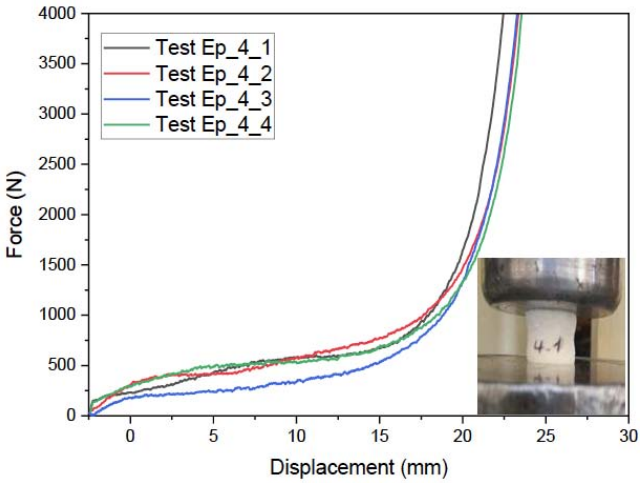

Figure 9: Force-displacement curve of polyurethane foams EP_04.

For the foam Ep_5, a 33.1 mm diameter open-cell polyurethane foam is converted by axial pressure at the stated level, and the forced displacement is noticed, as shown in Figure **10**. We note that the latter consists of three phases, thus identical to traditional foams. Other authors have documented this behavior [52]. The strength displacement curves were drawn for four samples of the same fifth foam composition to describe the mechanical behavior of the foam better to understand the difference between it and the rest of the samples and to ensure that the reported strength of the foam is similar to the second foam in terms of the plateau. The comparison of force movement for both load levels indicates correlations with a small rise in the maximum intensity of level 3 at 4000 N.

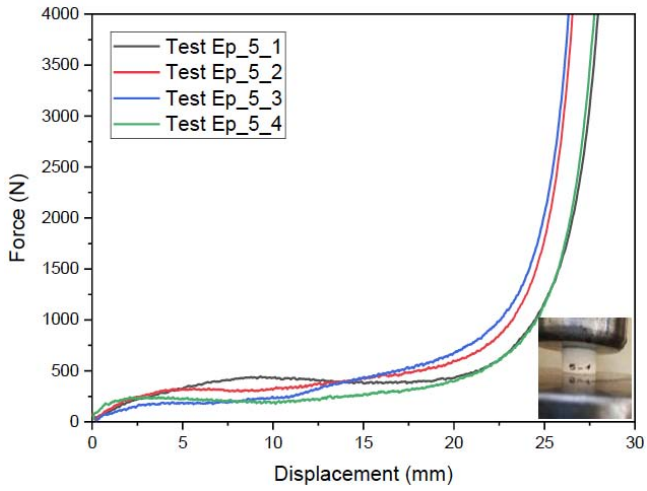

Figure 10: Force-displacement curve of polyurethane foams EP_05.

Figure **11** shows the force shift's action under the sixth foam's static compressive load, converting up to 80 % of the initial foam shape into pressure levels. The low dispersion of this behavior in a transformed foam by plane with a plateau accelerating to approximately 500 Newtons was recorded. It should also be noted that the dispersion at the maximum force is very large in two transformation levels, and in the case of level 3, which is a maximum of 4000 Newtons, the highest strength is reached.

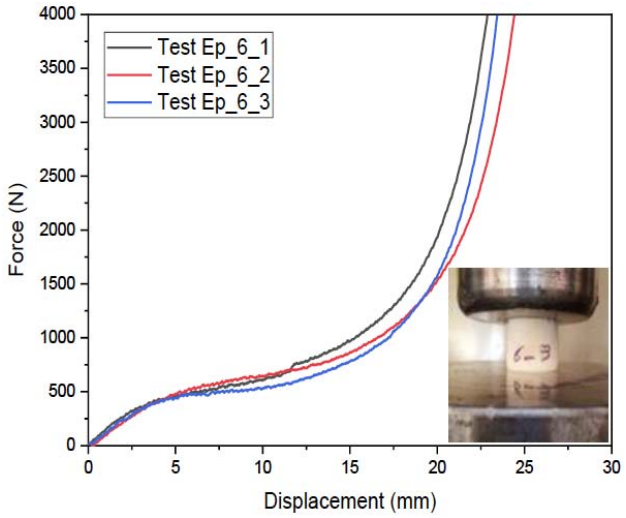

Figure 11: Force-displacement curve of polyurethane foams EP_06.

The comparison of the typical curves of transforming foams shows similarity in force shifting up to a change

of approximately 5 mm, which corresponds to a compression ratio of 40%. The strength displacement behavior of the second and fifth samples (see Figure **12**) is stronger, and the maximum strength at a pressure of 80 % is very strong for anti-shock applications. We note that the two samples contain alumina and bentonite, which helped to form an ideal structure to absorb high pressures. In the case of static compression of the pressurized mousse, the force/dislocation behavior is reported over three phases; this behavior is close to that of traditional molds. The average strength of the plateau is 200 Newtons with strong productivity of foaming tests. On the other hand, until the 20 mm displacement, the dispersion is very low and even greater, especially at the maximum force registered at the 25 mm displacement.

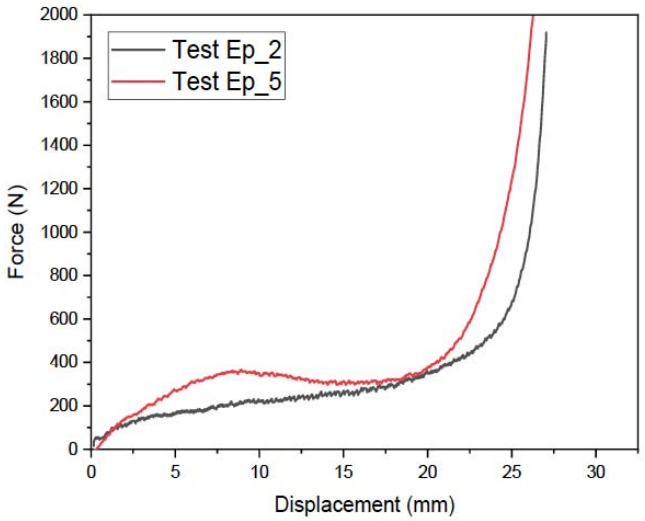

Figure 12: Curve force-displacement for comparison of EP_02 and EP_05 polyurethane foam.

Figure **12** shows a comparison between the second foam and the fifth foam transformed by the pressure plane, and the behavior is almost the same (superposition of curves) for the foam in the elastic plateau plane, especially at the displacement point of 17 mm. It should also be noted that the maximum force value of the second foam does not exceed 2000 Newtons. This could be related to the difference in the density of the fifth foam, which was 14 times the density of the second foam.

The mechanical characteristics of foams strongly depend on the density and structure of the cells (shape and size) and the percentage of open and closed cells. The foam may have a preferential orientation to the structure of the cells. Cells frequently appear elongated along the direction of expansion. By the way, as the density of the foam grows, the foam becomes less elastic, the height of the plate increases [53, 54], and the elongation of the plate decreases [55]. High-density foam is thus more resistant to applied stress than low-density foam. However, the composition of high-density foam results in low-stress densification. For rigid foams, the stress value decreases dramatically at the end of the tray. Rather than observing increased stress due to densification, the stress value decreases sharply at the end of the tray. This is when the cell walls rupture, and the foam structure collapses [56].

The fillers used can be bentonite or alumina, a reason for endurance. Adding particles smaller than the foam cells increases the value of the initial modulus in the strain-stress curve. On the other hand, if the dimensions of the added particles are larger than those of the cells, the reinforcement is ineffective [54]. Polyurethane foams consist of a mixture of rigid domains and soft domains. It has been found that inflation of temperature or humidity significantly deteriorates the mechanical properties of foams [57]. This loss of mechanical properties corresponds to a decrease in compressive strength. It is probably linked to splitting chains belonging to the rigid domains (urea and urethane bonds) and breaking hydrogen bonds [58]. Determining the apparent density (ρ) of the different polyurethane foams studied consists of weighing the samples with an accuracy of 0.01 g and calculating the volume of the test pieces (Figure **S11**). The average results obtained for untransformed polyurethane foams (original) are given in Table **3**.

3.2.2. Poisson Ratio Determination (v)

Two separate methods were employed to calculate the Poisson ratio of that polyurethane foam specimen while exposed to compression uniaxial. In the initial technique, getting images of the specimen at various compression ratios, the cross-sectional range is determined using picture processing techniques with MATLAB (Figure **S12**). On average, the Poisson's ratio

Table 5: Values Derived Experimentally from the Overall Compression Force of Polyurethane Foam

Polyurethane foams	EP_01	EP_02	EP_03	EP_04	EP_05	EP_06
Maximum compression force 80 % (N)	15024	1581	15679	15568	10391	18533

Table 6: Characteristics of Samples before and after Compression Tests

Polyurethane foam	Length (mm)	Length after compression (mm)	Diameter (mm)	Diameter after compression (mm)	Density (g/cm^3)	Density after compression (mm) (g/cm^3)
Ep_1_1	35.6	30	35.5	31	0.32	**0.5**
Ep_1_2	35.5	30.5	35.7	33	0.34	**0.46**
Ep_1_3	35.5	30	36.5	33	0.31	**0.45**
Ep_1_4	35.4	30	35.9	33.2	0.32	**0.44**
Ep_2_1	34.72	34.41	34.2	32.61	0.07	**0.08**
Ep_2_2	32.5	32.41	32.41	33.22	0.08	**0.07**
Ep_2_3	30.72	30.42	34	32.34	0.07	**0.08**
Ep_2_4	30	30	31.51	30.3	0.07	**0.07**
Ep_3_1	32.31	32	32.71	32.5	0.23	**0.23**
Ep_3_2	31.68	32.31	31.6	31	0.23	**0.24**
Ep_3_3	30.01	30	32	32.71	0.24	**0.22**
Ep_3_4	30.4	30	32	33	0.27	**0.26**
Ep_4_1	32.36	32.1	32.4	32.66	0.23	**0.23**
Ep_4_2	32.48	32.16	32.58	33	0.23	**0.22**
Ep_4_3	32.58	32	32.6	33.1	0.23	**0.22**
Ep_4_4	32.3	31	32	32.58	0.22	**0.23**
Ep_5_1	33.16	32.56	33.1	33.06	0.16	**0.16**
Ep_5_2	31.18	30.4	31.78	33.28	0.18	**0.17**
Ep_5_3	31	30.42	31.4	33.1	0.18	**0.17**
Ep_5_4	32.66	32	32.1	32.94	0.17	**0.17**
Ep_6_1	32.58	32.18	32.66	33.56	0.34	**0.32**
Ep_6_2	33.64	33.28	33.14	34	0.32	**0.31**
Ep_6_3	**35.6**	**32**	**32.48**	**33.36**	**0.34**	**0.32**

is determined based on the estimated areas. Foam samples are unusually compressed at a certain compression stage. Photos are taken at varying levels by compressing them with a compact camera placed on a tripod. Photos of 0 %, then 25 %, then 50 %, then 75 %, and 80 %. Digital pictures are processed by using the picture processing toolkit in MATLAB. The im2bw MATLAB command transforms initial images into grayscale, a picture with intensity. Then the grayscale images are transformed into black and white (Figure **13**) by thresholding binary images. If picture pixels have luminance below the minimum, the binary picture output has 0 (black) and 1 for most added pixels (white). Based on a visual study of initial and processed pictures, the threshold is 0,8. For each image, the background color white, calculated in pixels, is determined by the area occupied by the PUR foam [59]. For method two, digital images are used not to estimate the area but instead to estimate the ratio of lateral aspect and, thus, the Poisson ratio for the relative displacement of material points.

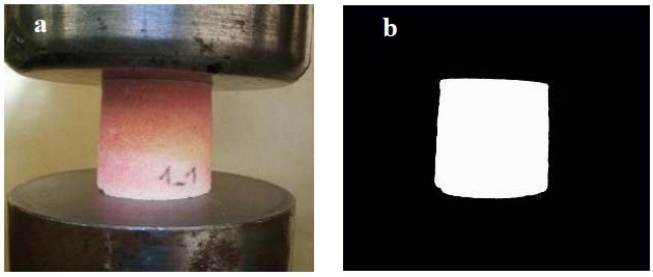

Figure 13: Uniaxial compression foam images in the vertical direction below 0%, 25%, 50%, 75%, and 80% of the pressing ratio.

The calculation of the Poisson ratio for the various samples is achieved through an imaging technique consisting of taking photographic images at certain compression rates and measuring the widths of these samples so that the Poisson's ratio can be identified

(see Figure **14**). However, exponential behavior demonstrates the evolution of the mechanical behaviors of negative Poisson-ratio foams [60].

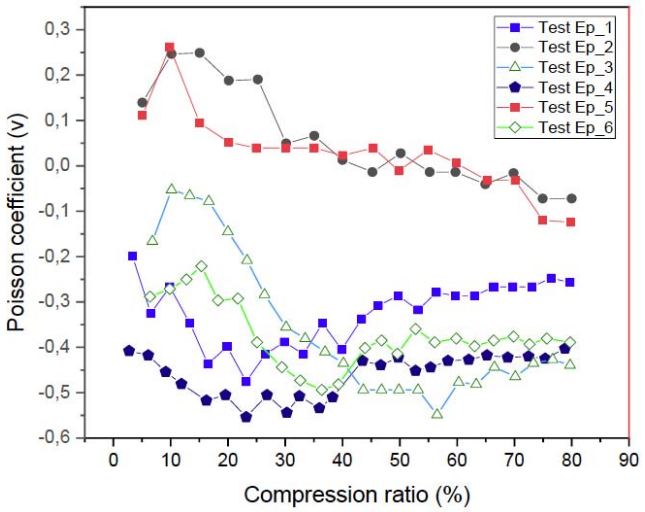

Figure 14: The Poisson ratio (v) difference according to the compression of the various foams tested.

The diameters of the test parts are determined according to the compression ratio of the various foams tested. This analysis is shown in Figure **14**. Poisson ratio variance (v) is based on the studied foam compression ratio. The second and fifth foams have overall positive Poisson ratios of 0.25 for a compression ratio of 10% and 15%, followed by a decrease with a compression ratio of up to 80% to -0.1% for the foam. The first, third, fourth, and sixth transformed foams have negative Poisson ratios, in the form of a plateau, very near the border of-0.25 to-0.45, with a compression rate of between 50 and 80 %. This is caused by the microscopic transformations in the samples of materials that determine the durability of the cytoskeleton of the polyurethane foam, leading to the unique shape of the ribs of elongated or compact cells. The result is a negative Poisson ratio. With Poisson-0.55 obtained for the compression rate of 25 %, the fourth foam has a slightly greater degree of permittivity, while for the first foam, this coefficient is just-0.48 for the same compression ratio. For the third foam, the compression ratio is-0.55 at 57.5%, and we have also reported a Poisson coefficient of-0.5 for the sixth foam, with a pressure ratio of 37.5%. Even if the core ratio of Poisson is positive [61], the Poisson ratio can become harmful. Brander and Lakes [62] Poisson's coefficient-0.5 for polyurethane foams is very similar to the sixth foam of this research.

The experimental results are consistent with recent scientific references. For example, Wen *et al*. [63] studied the dynamic constitutive model of high-density rigid polyurethane foam subjected to impact loading. They found that the Poisson's ratio of the foam decreased with increasing strain rate and became negative at high strain rates. They attributed this phenomenon to the microstructural changes in the foam cells, such as cell wall buckling and hinge rotation. Liu *et al*. [64] studied the mechanical properties of polyurethane-enhanced triply periodic minimal composite structures inspired by rachis microstructure and found that the Poisson's ratio of the composite structures was negative and tunable by changing the rachis angle and thickness. They explained that the negative Poisson's ratio was due to the deformation mechanism of bending-dominated auxetic behavior.

However, some scientific references also report different findings from the experimental results. For example, Rahimidehgolan *et al*. [65] investigated the influence of specimen profile size and thickness on the dynamic compressive behavior of rigid PVC foams. They found that the Poisson's ratio of the foams increased with increasing strain rate and became positive at high strain rates. They suggested that this was due to the densification and compaction of the foam cells under high strain rates. Koohbor and Youssef [66] reviewed the polymeric foams and their nanocomposite derivatives for shock absorption. They found that most polymeric foams had positive Poisson's ratios static and dynamic loading conditions [67]. They stated that this was due to the elastic recovery and resilience of the foam cells.

Therefore, it can be seen that there is no universal trend for Poisson's ratio of polyurethane foams under different loading conditions. The Poisson's ratio depends on foam density, cell morphology, strain rate, loading direction, and microstructural changes. The experimental results presented in this paper provide valuable insights into the auxetic behavior of polyurethane foams with different topologies and compression ratios. However, more studies are needed to understand the underlying mechanisms and factors affecting Poisson's polyurethane foams ratio in different scenarios.

The effect of temperature on the mechanical properties of polyurethane foams is significant and complex. [68], increasing temperature generally leads to an increase in pore size, a decrease in density, and a decrease in the mechanical properties of polyurethane foams. However, different temperatures affect different stages

Table 7: The Table Shows the Data from Different References on Various Parameters and Properties of Polyurethane Foams

Reference	Method	Parameters	Properties	Comparison with our results
Widdle Jr *et al*., 2008 [59]	Image processing and area estimation	Uniaxial compression ratio	Poisson's ratio (0.15 - 0.45)	A similar range of Poisson's ratio for some foams but a different trend with an increasing compression ratio
Vaz & Fortes, 2001 [60]	Finite element simulation and cell collapse analysis	Uniaxial compression ratio	Poisson's ratio (-0.2 - 0.2)	A similar range of Poisson's ratio for some foams but a different trend with an increasing compression ratio
Yang *et al*., 2003 [61]	Finite element simulation and geometric analysis	Uniaxial compression ratio, cell angle, cell size, cell thickness	Poisson's ratio (-0.5 - 0.5)	A similar range of Poisson's ratio for some foams but different dependence on geometric parameters
Brandel & Lakes, 2001 [62]	Thermo-mechanical processing and re-entrant transformation	Uniaxial compression ratio	Poisson's ratio (-0.25 - 0.45)	A similar range of Poisson's ratio for some foams, but different mechanism of re-entrant transformation
Wen *et al*., 2023 [63]	Split Hopkinson pressure bar test and dynamic constitutive model	Impact loading, strain rate, microstructural changes	Poisson's ratio (-0.1 - 0.3)	Similar range and trend of Poisson's ratio for high-density rigid polyurethane foam under impact loading
Liu *et al*., 2023 [64]	Finite element simulation and experimental testing	Uniaxial tension and compression, rachis angle, rachis thickness	Poisson's ratio (-0.4 - 0), compressive modulus, tensile modulus	Similar range and trend of Poisson's ratio for polyurethane-enhanced triply periodic minimal composite structures under uniaxial tension and compression
Rahimidehgolan *et al*., 2023 [65]	Split Hopkinson pressure bar test and image processing	Impact loading, strain rate, specimen profile size, specimen thickness, densification, compaction	Poisson's ratio (0.1 - 0.4)	Different ranges and trends of Poisson's ratio for rigid PVC foams under impact loading
Koohbor & Youssef, 2023 [66]	Literature review and analysis	Static and dynamic loading, elastic recovery, resilience	Poisson's ratio (positive), compressive strength, tensile strength, energy absorption	Different range of Poisson's ratio for most polymeric foams under static and dynamic loading conditions
K. O. Park *et al*., 2005 [67]	Cellular structure transformation and image processing	Uniaxial compression ratio, volumetric compression ratio, cell wall buckling, hinge rotation	Poisson's ratio (-3.4 - 0), deformability, resilience	A similar mechanism of cell wall buckling and hinge rotation for negative Poisson's ratio behavior, but different range of Poisson's ratio for polyurethane foam with a negative Poisson's ratio
Wang *et al*., 2022 [68]	Literature review and analysis	Temperature, pore size, density, cell morphology, phase separation	Thermal conductivity, compressive strength, tensile strength, elastic modulus, etc.	Different effects of temperature on the mechanical properties of polyurethane foams
Saint-Michel *et al*., 2006 [69]	Experimental testing and modeling	Bentonite or alumina particles, filler size, filler compatibility, filler dispersion	Compressive strength, initial modulus, stress-strain curve, etc.	Different effects of filler type and size on the mechanical properties of polyurethane foams
Petrů *et al*., 2017 [69]	Experimental testing and numerical modeling	Density, cell morphology, soft and rigid domains	Stiffness, strength, elasticity, energy absorption	A similar effect of density on the mechanical properties of polyurethane foams
Abedini *et al*., 2022 [71]	Experimental testing and image analysis	Chemical composition, cellular structure, compression ratio	Poisson's ratio (-0.55 - 0.25), compressive modulus (1 - 10 MPa), stress-strain curve	Our results are based on this reference
WO1999025530A1 - Scale-up of Negative Poisson's Ratio Foams - Google Patents, n.d. [72]	Mold assembly and heat treatment	Volumetric compression ratio (1 - 10)	Poisson's ratio (-0.5 - -1), deformability (10% - 100%), resilience (90% - 100%)	Different ranges and trends of Poisson's ratio for negative Poisson's ratio foams with different volumetric compression ratios
Y. J. Park & Kim, 2013 [73]	Scaffold fabrication and cell culture	Negative Poisson's ratio scaffold	Negative Poisson's ratio scaffold (-0.55), chondrocyte proliferation (2 - 4 times), collagen production (1.5 - 2 times)	Different applications of negative Poisson's ratio polyurethane scaffold for articular cartilage tissue engineering

of foam formation and service. The effect of filler type and size on the mechanical properties of polyurethane foams depends on the filler particles' compatibility and dispersion in the polymer matrix. Adding bentonite or alumina particles can improve polyurethane foams' thermal stability, and fire resistance also affects their mechanical properties in different ways [69]. Adding particles smaller than the foam cells can increase the initial modulus in the stress-strain curve while adding particles larger than the cells can reduce the reinforcement effect. Moreover, adding alumina particles can increase the compressive strength at low strain levels, while adding bentonite particles can increase the compressive strength at high strain levels.

The effect of density on the mechanical properties of polyurethane foams is related to the foam architecture and cell wall composition. Increasing density can increase the stiffness and strength of polyurethane foams but also reduce their elasticity and energy absorption capacity [70]. Moreover, increasing density can change the relative contribution of soft domains (polyol segments) and rigid domains (urea and urethane bonds) to the mechanical behavior of polyurethane foams. The 2 + 1 phase model can better describe this behavior than the Gibson and Ashby approach, as it considers both phases separately.

The experimental results show that the Poisson ratio of polyurethane foams depends on the chemical composition, the cellular structure, and the compression ratio. Some foams have positive Poisson ratios, meaning they become thinner when stretched and thicker when compressed, as expected for most materials. However, some foams have negative Poisson ratios, which means they behave oppositely, becoming thicker when stretched and thinner when compressed. This is attributed to the microscopic transformations in the cell ribs of the foams, which can buckle or elongate depending on the applied stress [71]. The text also shows that some foams have very low or high negative Poisson ratios lost to the theoretical limits of -0.5 and -1.0, respectively [72]. These values indicate that the foams have very high deformability and resilience, which are useful for shock absorption and energy dissipation applications [73].

Table **7** shows the data from different references on various parameters and properties of polyurethane foams. We can use this table to compare and contrast the results from different studies and understand the factors and mechanisms that affect the mechanical behavior of polyurethane foams.

3.3. Microstructural Characterization

3.3.1. Scanning Electron Microscope (SEM)

As presented in Figure **15**, the electron microscope image was taken immediately after the drop experiment. The spastic fracture of the alumina-reinforced polyurethane foam Ep_05 appeared immediately after the blast damage. It has been found that this foam first generates a compressive deformation onward load-carrying bearing, then appears to cause crop and tear damage along the direction of the fall. We note that after hours, the foam returns to its normal state, but the shock effects do not appear to the naked eye and must be examined with an electron microscope to monitor the evolution of the impact of the fall experiment.

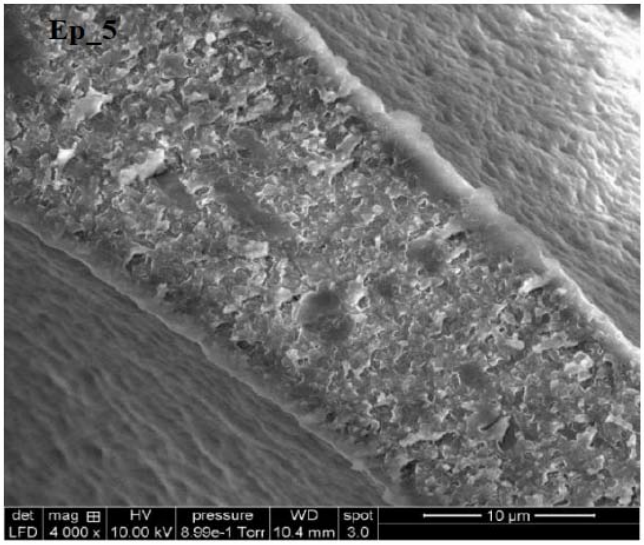

Figure 15: Polyurethane foam fracture surfaces Ep_05 after a burst inspection.

Figure **15** shows the foam cells loaded with different proportions of bentonite; after compressing, the elongation of the cells appears parallel to the falling hammer. We also note a change in the reinforcement content of bentonite as the distribution appears to be heterogeneous with the foam cells. It is believed that strengthening the bentonite can greatly improve the force of the blast as the latter is not affected by the force of the impact. The main reason is that the reinforced bentonite added to the polyurethane foam can increase the neogenesis between the foamed cells, and the number of cells becomes higher per unit region.

When the loaded polyurethane foam is subjected to force, such cells spread and effectively consume the force of the blast. In comparison, we note that alumina-

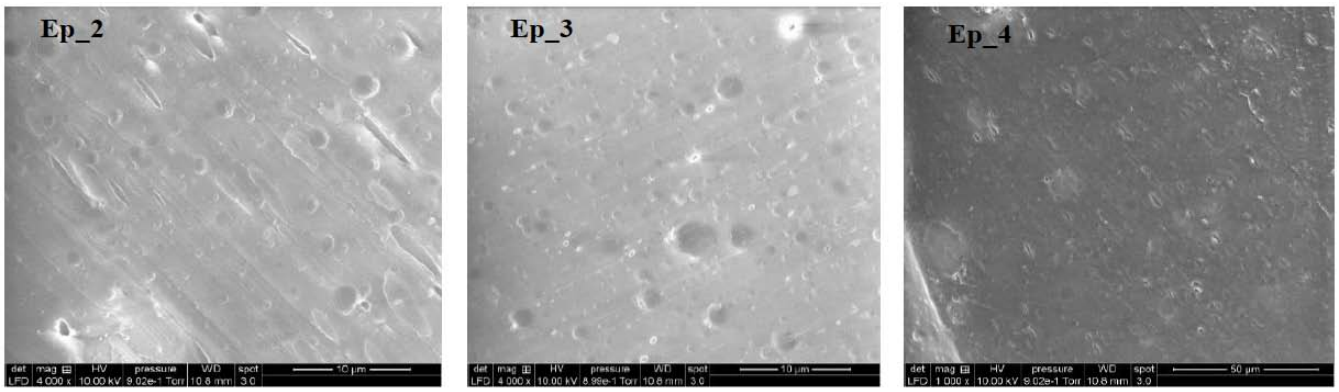

Figure 16: SEM images of polyurethane foam cells Ep_2, Ep_3, and Ep_4 show the diffusion of foam cells loaded with different proportions of bentonite.

loaded foam has a much higher burst strength than bentonite-loaded. That is because bentonite is less dense than alumina, and with the same weight ratio, the amount of alumina is greater than that of bentonite. Thus, the alumina in the polyurethane foam is evenly distributed, and the explosive pressure is easily spread along the urethane chain. Loads exceeding 11% by weight are difficult to distribute evenly. They will be subjected to accumulation in a polyurethane mixture. In the end, polyurethane foams adding 10% alumina by weight have an ideal bursting force of 150 N.

The calculated apparent density of the prepared polyurethane foams was between (0.15 and 0.43 g/cm^3). Although the densities of the same formula are very related from a functional perspective, it has also been found that the standard deviation of polyurethane foams containing loads of bentonite and alumina has a value of twice the standard deviation of load-free foams. The findings reveal that integrating loads within the foam results in a somewhat heterogeneous formation.

SEM images of the polyurethane foam microstructure from the second, third, and fourth samples loaded with different proportions of bentonite are shown in Figure **16**. The polyurethane had an asymmetric expansion, and the cell was slightly extended within the expansion region. This investigation is demonstrated by the fact that this polyurethane foam was formed into a rigid structure.

In the statistical study of the second bentonite-loaded polyurethane foam cell volume (Figure **16**), it was realized that the magnitude of the cells parallel to the expansion direction was 616 ± 106 µm. The cell magnitude in the vertical direction was 370 ± 60 µm. On the contrary, the volume of the alumina-loaded foam cell (Figure **15**) showed low volume in both directions. That is, the mesh magnitude in the longitudinally also vertical directions was 450 ± 144 µm and 243 ± 60 µm, respectively. This drop was observed in the size of other nano-reinforced [41].

We can also see in Figure **17** the distribution of alumina in the fifth formula polyurethane foam. These loads are distributed in an untidy but homogeneous manner. By comparison with the distribution of bentonite in the polyurethane matrix, we notice that the distribution of alumina is better. This is due to the nanometric scale's smaller radius of alumina than bentonite. Alumina causes a slight variation in cell orientation reverently to growth direction 10-15, and this may be due to the action of alumina for thixotropic reinforcing, which leads to a changing viscosity prerogative and an increase in the temperature during elevation [74].

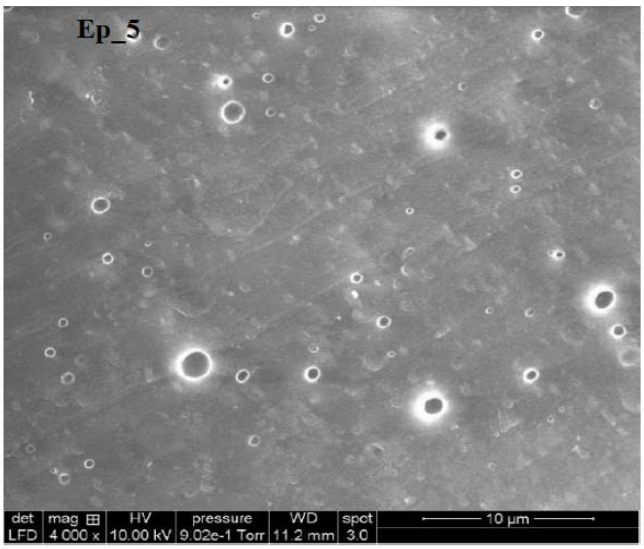

Figure 17: SEM images of Ep_5 polyurethane foam cells, showing the distribution of alumina in a polyurethane matrix.

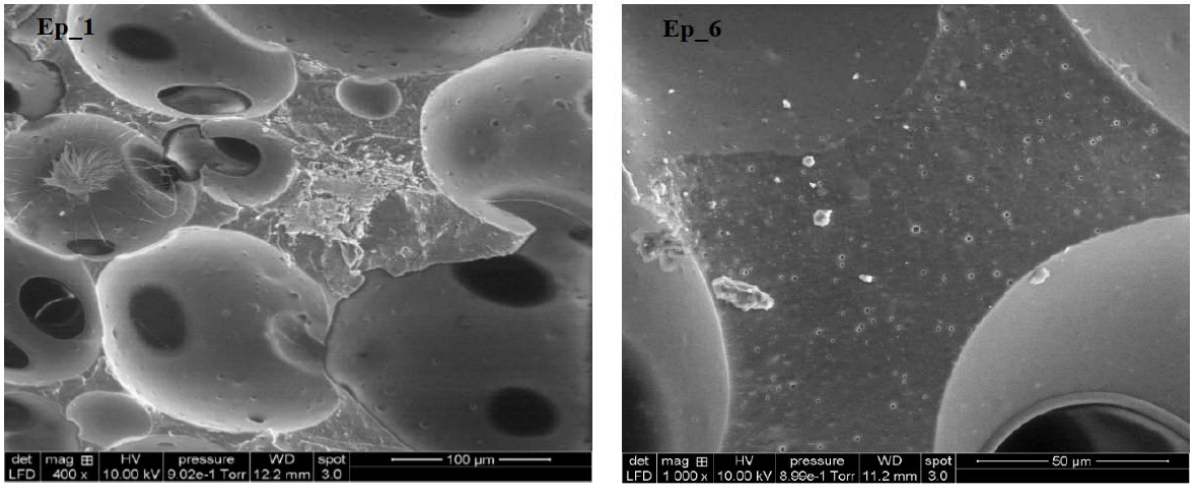

Figure 18: SEM pictures of polyurethane foam cells Ep_1 and Ep_6, showing the cross-section of the abutment of the alveolar structure.

Figure **18** shows the cross-section of the first and sixth polyurethane foam supports. A rough and partially smooth surface can be observed where these cells appear partially open, allowing them to absorb shock effectively. This shows that additional breakdown levels are created when cells are broken down [41].

CONCLUSIONS

The results and scanning electron microscope images show that loads of bentonite and alumina strengthen the foam structure. The effectiveness of shock absorption was related to a specific proportion of the loads.

The mechanical characterization of polyurethane foam of a certain density aims to calibrate the usability of the foam experimentally in the laboratory before its use as a non-lethal weapon. Based on these alveolar materials, these last warheads should be able to stall the target without causing permanent injury or fatal outcomes. The experimental results are presented for mechanical tests. The dynamic tests are performed by the drop Drop weight machine we designed and manufactured.

Six separate series of polyurethane foams have been prepared and subsequently tested under static loading with a sample range divided into four samples for pressure testing of each series. The completion of these tests enables the following conclusions to be drawn:

- The mechanical action (force-displacement) occurs in three phases at the static pressure in the second and fifth polyurethane foams; a linear phase shadowed by a plateau and then a condensed phase where the strength is rapidly increased by increasing displacement. The linear foam process is tiny. The conversion rate effect determines the foam's movement since the fifth foam's overall compressive strength is greater than that of the second foam. The second and fifth foams have the highest Poisson positive ratios of 0.25 to 10 % and 15 % of corresponding compression ratios.

- The first, third, fourth, and sixth foams have negative Poisson ratios (acoustic), which are very similar to a plateau, in the order of-0.25 to-0.45 for a compression ratio of 50 to 80%. The dispersion reported in the results is primarily due to the foam's shape and the spontaneous structural changes in cell dimensions and defects.

- The microstructural analysis demonstrated the open-cell nature of the foam produced. Also, an improvement in the production process is necessary to ensure better respectability of the characteristics of the foams studied.

The results of the compression tests showed the typical behavior of viscoelastic materials in three phases: linear elastic deformation, plateau, and densification.

CONFLICTS OF INTEREST

The authors note that the investigation was carried out without any corporate or financial arrangements, which could be perceived as a conflict.

ACKNOWLEDGEMENTS

I sincerely thank the Director of Research and postgraduate training at EMP, Prof. Ouali Hamid, Teaching & Research Unit in Applied Mechanics at EMP. I thank Prof. SAFIDINE Zitouni, Prof. BOUDIAF Achraf, Prof. DUCHET-RUMEAU Jannick, and Prof. GERARD Jean-François for the precious lessons and the wonderful advice you have given me in understanding various aspects of the research. I'm thankful to the Ecole Military Polytechnique (EMP) and the Ministry of Higher Education and Scientific Research (MESRS) for letting me do this job and giving me training and financial and emotional support.

FUNDING

This research was funded by the General Directorate of Scientific Research and Technological Development (DGRSDT). The Ministry of Higher Education and Scientific Research (MESRS) by Grant number #Projects PNE/2019EMP.

AUTHOR CONTRIBUTIONS

Formal analysis, Writing - Original Draft Preparation, Funding acquisition, Resources, Review and Editing, Software, Investigation, visualization BN; Data Curation, Conceptualization, and methodology MAL.

SUPPORTING INFORMATION

The supporting information can be downloaded from the journal website along with the article.

REFERENCES

[1] Maiolino P, Galantini F, Mastrogiovanni F, Gallone G, Cannata G, Carpi F. Soft dielectrics for capacitive sensing in robot skins: Performance of different elastomer types. Sens Actuators A Phys 2015; 226: 37-47. https://doi.org/10.1016/j.sna.2015.02.010

[2] Patten WN, Sha S, Mo C. A vibration model of open celled polyurethane foam automotive seat cushions. J Sound Vib 1998; 217: 145-61. https://doi.org/10.1006/jsvi.1998.1760

[3] Noureddine B, Zitouni S, Achraf B. A new study of dynamic mechanical analysis and the microstructure of polyurethane foams filled. Turk J Chem 2022; 46: 814-34. https://doi.org/10.3906/kim-2108-53

[4] Goldsmith W, Frasier JT. Impact: The Theory and Physical Behavior of Colliding Solids. E. Arnold 1961; 28. https://doi.org/10.1115/1.3641808

[5] Sung DK. Modeling and analysis of a nonlinear elastomer impact model with damping mechanism. IECON Proceedings (Industrial Electronics Conference) 1991; 1: 609-12. https://doi.org/10.1109/iecon.1991.239217

[6] Thornhill RJ, Smith CC. Impact Force Prediction Using Measured Frequency Response Functions. American Society of Mechanical Engineers (Paper) 1981.

[7] Boumdouha N, Duchet-Rumeau J, Gerard J-F, Eddine Tria D, Oukara A. Research on the Dynamic Response Properties of Nonlethal Projectiles for Injury Risk Assessment. ACS Omega 2022. https://doi.org/10.1021/acsomega.2c06265

[8] Gung JL, Huang HW, Chiu TC, Lai YS. Application of viscoelastic model for simulating process-induced warpage of ball grid array packages. IMPACT Conference 2009 International 3D IC Conference - Proceedings, IEEE 2009; pp. 6-9. https://doi.org/10.1109/IMPACT.2009.5382296

[9] Sherwood JA, Frost CC. Constitutive modeling and simulation of energy absorbing polyurethane foam under impact loading. Polym Eng Sci 1992; 32: 1138-46. https://doi.org/10.1002/pen.760321611

[10] Boehme B, Roellig M, Wolter KJ. Material characterization of organic packaging materials to increase the accuracy of FEM based stress analysis. Proceedings - 2008 2nd Electronics Systemintegration Technology Conference, ESTC, IEEE; 2008; pp. 459-62. https://doi.org/10.1109/ESTC.2008.4684391

[11] Ionescu M. Chemistry and Technology of Polyols for Polyurethanes, 2nd Edition Chemistry and Technology of Polyols for Polyurethanes, 2nd Edition. iSmithers Rapra Publishing 2016; 2.

[12] Sharmin E, Zafar F. Chapter 1, Polyurethane: An Introduction. Polyurethane; Zafar F, Sharmin E, Eds. INTECH: Rijeka, Croatia 2012; 3-6.

[13] Prisacariu C. Polyurethane Elastomers: From Morphology to Mechanical Aspects. Springer Science & Business Media 2011.

[14] Szycher M. Szycher's handbook of polyurethanes. CRC press 1999; 37. https://doi.org/10.5860/choice.37-1570

[15] Król P. Linear polyurethanes: synthesis methods, chemical structures, properties and applications. CRC Press 2008.

[16] Ashida K. Polyurethane and Related Foams. CRC press 2006. https://doi.org/10.1201/9780203505991

[17] Lee ST, Ramesh NS. Polymeric foams: Mechanisms and materials. CRC press 2004.

[18] Luo X, Xiao Y, Wu Q, Zeng J. Development of high-performance biodegradable rigid polyurethane foams using all bioresource-based polyols: Lignin and soy oil-derived polyols. Int J Biol Macromol 2018; 115: 786-91. https://doi.org/10.1016/j.ijbiomac.2018.04.126

[19] Das S, Heasman P, Ben T, Qiu S. Porous Organic Materials: Strategic Design and Structure-Function Correlation. Chem Rev 2017; 117: 1515-63. https://doi.org/10.1021/acs.chemrev.6b00439

[20] Wellnitz CC, Miskioglu I, Zawisza JD. Assessment of extruded polystyrene foam for sandwich composite applications. International SAMPE Technical Conference 2008.

[21] Titow WV. PVC plastics: properties, processing, and applications. Springer Science & Business Media 2012.

[22] Boumdouha N, Safidine Z, Boudiaf A, Djalel Eddine T, Oukara A. Élaboration et caractérisation mécanique des mousses polyuréthanes modifiés. Fourth International Conference on Energy, Materials, Applied Energetics and Pollution ICEMAEP2018, Constantine, Algeria: Université Frères Mentouri Constantine 1 2018; pp. 136-42. https://doi.org/10.4000/cybergeo.23797

[23] Miller M. Polymers in Cementitious Materials. iSmithers Rapra Publishing 2005.

[24] Saxena PK, Raut KG, Srinivasan SR, Sivaram S, Rawat RS, Jain RK. Polyurethane waterproofing coating for building applications. Constr Build Mater 1991; 5: 208-10. https://doi.org/10.1016/0950-0618(91)90052-M

[25] Sharmin E, Zafar F. Polyurethane: an introduction. Polyurethane 2012: 3-16.

[26] Yi J, Boyce MC, Lee GF, Balizer E. Large deformation rate-dependent stress-strain behavior of polyurea and polyurethanes. Polymer (Guildf) 2006; 47: 319-29. https://doi.org/10.1016/j.polymer.2005.10.107

[27] Rocco JAFF, Lima JES, Lourenço VL, Batista NL, Botelho EC, Iha K. Dynamic mechanical properties for polyurethane elastomers applied in elastomeric mortar. J Appl Polym Sci 2012; 126: 1461-7. https://doi.org/10.1002/app.36847

[28] Nwosu SN, Hui D, Dutta PK. Dynamic mode II delamination fracture of unidirectional graphite/epoxy composites. Compos B Eng 2003; 34: 303-16. https://doi.org/10.1016/S1359-8368(02)00039-2

[29] Demir H, Sipahioğlu M, Balköse D, Ülkü S. Effect of additives on flexible PVC foam formation. J Mater Process Technol 2008; 195: 144-53. https://doi.org/10.1016/j.jmatprotec.2007.04.123

[30] Xia F, Wu X qing. Study on impact properties of through-thickness stitched foam sandwich composites. Compos Struct 2010; 92: 412-21. https://doi.org/10.1016/j.compstruct.2009.08.016

[31] Sachse S, Poruri M, Silva F, Michalowski S, Pielichowski K, Njuguna J. Effect of nanofillers on low energy impact performance of sandwich structures with nanoreinforced polyurethane foam cores. Journal of Sandwich Structures and Materials 2014; 16: 173-94. https://doi.org/10.1177/1099636213512497

[32] Lascoup B, Aboura Z, Khellil K, Benzeggagh M. Impact response of three-dimensional stitched sandwich composite. Compos Struct 2010; 92: 347-53. https://doi.org/10.1016/j.compstruct.2009.08.012

[33] Marsavina L, Linul E, Voiconi T, Sadowski T. A comparison between dynamic and static fracture toughness of polyurethane foams. Polym Test 2013; 32: 673-80. https://doi.org/10.1016/j.polymertesting.2013.03.013

[34] Baral N, Cartié DDR, Partridge IK, Baley C, Davies P. Improved impact performance of marine sandwich panels using through-thickness reinforcement: Experimental results. Compos B Eng 2010; 41: 117-23. https://doi.org/10.1016/j.compositesb.2009.12.002

[35] Boumdouha N, Safidine Z, Boudiaf A, Duchet-Rumeau J, Gerard J-F. Experimental study of the dynamic behaviour of loaded polyurethane foam free fall investigation and evaluation of microstructure. The International Journal of Advanced Manufacturing Technology 2022. https://doi.org/10.1007/s00170-022-08963-1

[36] Boumdouha N, Safidine Z, Boudiaf A. Preparation of Nonlethal Projectiles by Polyurethane Foam with the Dynamic and Microscopic Characterization for Risk Assessment and Management. ACS Omega 2022. https://doi.org/10.1021/acsomega.2c01736

[37] Noureddine B, Zitouni S, Achraf B, Houssém C, Jannick D-R, Jean-François G. Development and Characterization of Tailored Polyurethane Foams for Shock Absorption. Applied Sciences 2022; 12: 2206. https://doi.org/10.3390/app12042206

[38] Boumdouha N. Project Polytechnique Reporting. Lyon, French 2022. https://doi.org/10.13140/RG.2.2.20872.08964

[39] Boumdouha N, Safidine Z, Boudiaf A, Oukara A, Tria DE. Élaboration et caractérisation mécanique des mousses polymères : application aux projectiles non létaux. 11 th Days of Mechanics JM'11-EMP, Bordj El Bahri, Algeria: Military Polytechnic School (EMP) 2011; pp. 24-33. https://doi.org/10.4000/books.oep.332

[40] Meram A. Dynamic characterization of elastomer buffer under impact loading by low-velocity drop test method. Polym Test 2019; 79: 106013. https://doi.org/10.1016/j.polymertesting.2019.106013

[41] Fausett L. Fundamentals of Neural Network: Architectures, Algorithms, and Applications. Pearson Education India 1994; C-18.

[42] Boumdouha N, Safidine Z, Boudiaf A, Oukara A, Tria DE, Louar A. Mechanical and microstructural characterization of polyurethane foams. 8th Chemistry days JCh8-EMP, Bordj El Bahri, Algeria: Military Polytechnic School (EMP) 2019; p. 169. https://doi.org/10.4000/cybergeo.24732

[43] Boumdouha N, Safidine Z, Boudiaf A, Oukara A, Tria DE, Louar MA. Manufacture of polyurethane foam with a certain density. The International Conference on Recent Advances in Robotics and Automation ICRARE'18, Monastir - Tunisia: CES International Joint Conferences 2018; pp. 21-30. https://doi.org/10.4000/cybergeo.24737

[44] ASTM D. Standard test method for flexible cellular materials-slab, bonded, and molded urethane foams, American Society for Testing and Materials Philadelphia, PA 2005.

[45] Gibson LJ, Ashby MF. Cellular solids: structure and properties. Cambridge university press 1999.

[46] Saltykov SA. Stereometric metallography, 2nd edition, translation. Metallurgizdat, Moscow 1958; 267.

[47] Noureddine B, Achraf B, Zitouni S. Mechanical and chemical characterizations of filled polyurethane foams used for non-lethal projectiles. 10 the European Symposium on Non-Lethal Weapons EWG-NLW, Brussels, Belgium: Royal Military Academy 2019; p. 68. https://doi.org/10.4000/cybergeo.24738

[48] Boumdouha N, Safidine Z, Boudiaf A. Experimental Study of Loaded Foams During Free Fall Investigation and Evaluation of Microstructure. The International Journal of Advanced Manufacturing Technology 2021. https://doi.org/10.21203/rs.3.rs-792400/v1

[49] Bezazi A, Scarpa F. Mechanical behaviour of conventional and negative Poisson's ratio thermoplastic polyurethane foams under compressive cyclic loading. Int J Fatigue 2007; 29: 922-30.

[50] Gravade M, Ouisse M, Collet M, Scarpa F, Bianchi M, Ichchou M. Auxetic transverse isotropic foams: from experimental efficiency to model correlation 2012.

[51] Bianchi M, Scarpa F, Smith CW. Shape memory behaviour in auxetic foams: mechanical properties. Acta Mater 2010; 58: 858-65.

[52] Frioui N, Bezazi A, Remillat C, Scarpa F, Gomez JP. Viscoelastic and compression fatigue properties of closed cell PVDF foam. Mechanics of Materials 2010; 42: 189-95.

[53] Gong L, Kyriakides S, Jang W-Y. Compressive response of open-cell foams. Part I: Morphology and elastic properties. Int J Solids Struct 2005; 42: 1355-79.

[54] Saint-Michel F, Chazeau L, Cavaillé J-Y. Mechanical properties of high density polyurethane foams: II Effect of the filler size. Compos Sci Technol 2006; 66: 2709-18.

[55] Saha MC, Mahfuz H, Chakravarty UK, Uddin M, Kabir ME, Jeelani S. Effect of density, microstructure, and strain rate on compression behavior of polymeric foams. Materials Science and Engineering: A 2005; 406: 328-36.

[56] Jin H, Lu W-Y, Scheffel S, Hinnerichs TD, Neilsen MK. Full-field characterization of mechanical behavior of polyurethane foams. Int J Solids Struct 2007; 44: 6930-44.

[57] Dounis DV, Wilkes GL. Structure-property relationships of flexible polyurethane foams. Polymer (Guildf) 1997; 38: 2819-28.

[58] Moreland JC, Wilkes GL, Turner RB. Viscoelastic behavior of flexible slabstock polyurethane foams: Dependence on temperature and relative humidity. I. Tensile and compression stress (load) relaxation. J Appl Polym Sci 1994; 52: 549-68.

[59] Widdle Jr RD, Bajaj AK, Davies P. Measurement of the Poisson's ratio of flexible polyurethane foam and its influence on a uniaxial compression model. Int J Eng Sci 2008; 46: 31-49.

[60] Vaz MF, Fortes MA. Simulation of cell collapse in the compression of non-uniform cellular solids. Scr Mater 2001; 45: 375-82.

[61] Yang DU, Lee S, Huang FY. Geometric effects on micropolar elastic honeycomb structure with negative Poisson's ratio using the finite element method. Finite Elements in Analysis and Design 2003; 39: 187-205.

[62] Brandel B, Lakes RS. Negative Poisson's ratio polyethylene foams. J Mater Sci 2001; 36: 5885-93.

[63] Wen Y, Lai Z, Ma J, Liu H, Wang Y, Chi H, *et al*. A dynamic constitutive model for high-density rigid polyurethane foam subjected to impact loading. Constr Build Mater 2023; 387: 131642. https://doi.org/10.1016/J.CONBUILDMAT.2023.131642

[64] Liu R, Yao G, Sha L, Yu Z, Liang P, Han C, *et al*. Study on mechanical properties of polyurethane-enhanced triply periodic minimal composite structures inspired by rachis microstructure. Compos Sci Technol 2023; 242: 110197. https://doi.org/10.1016/J.COMPSCITECH.2023.110197

[65] Rahimidehgolan F, Magliaro J, Altenhof W. Influence of specimen profile size and thickness on the dynamic compressive behavior of rigid PVC foams. Int J Impact Eng 2023; 179: 104676. https://doi.org/10.1016/J.IJIMPENG.2023.104676

[66] Koohbor B, Youssef G. Polymeric Foams and Their Nanocomposite Derivatives for Shock Absorption. Multifunctional Polymeric Foams 2023. https://doi.org/10.1201/9781003218692-9

[67] Park KO, Park JC, Choi JB, Lee SJ, Choi HH, Kim JK. Polyurethane Foam with a Negative Poisson's Ratio for Diabetic Shoes. Key Eng Mater 2005; 288-289: 677. https://doi.org/10.4028/WWW.SCIENTIFIC.NET/KEM.288-289.677

[68] Wang J, Zhang C, Deng Y, Zhang P. A Review of Research on the Effect of Temperature on the Properties of Polyurethane Foams. Polymers 2022; 14: 4586. https://doi.org/10.3390/POLYM14214586

[69] Saint-Michel F, Chazeau L, Cavaillé J-Y, Chabert E. Mechanical properties of high density polyurethane foams: I. Effect of the density. Compos Sci Technol 2006; 66. https://doi.org/10.1016/j.compscitech.2006.03.009ï

[70] Petrů M, Novák O, Petrů M, Novák O. Measurement and Numerical Modeling of Mechanical Properties of Polyurethane Foams. Aspects of Polyurethanes 2017. https://doi.org/10.5772/INTECHOPEN.69700

[71] Abedini NHZ, Nourani A, Mohseni M, Hosseini N, Norouzi S, Bakhshayesh PR. Effects of geometrical and processing parameters on mechanical properties of auxetic polyurethane foams. SN Appl Sci 2022; 4: 1-16. https://doi.org/10.1007/S42452-022-05042-8/FIGURES/12

[72] WO1999025530A1 - Scale-up of negative poisson's ratio foams - Google Patents n.d. https://patents.google.com/patent/WO1999025530A1/en (accessed August 10, 2023).

[73] Park YJ, Kim JK. The effect of negative Poisson's ratio polyurethane scaffolds for articular cartilage tissue engineering applications. Advances in Materials Science and Engineering 2013; 2013. https://doi.org/10.1155/2013/853289

[74] Alsakarneh A, Moore L, Barrett J. Numerical modelling and optimization of an electronic system embedded in multi-layered viscoelastic materials under shock loads. 2011 12th Int. Conf. on Thermal, Mechanical and Multi-Physics Simulation and Experiments in Microelectronics and Microsystems, EuroSimE 2011, IEEE 2011; pp. 1-8. https://doi.org/10.1109/ESIME.2011.5765825